Original Article
ISSN (Online): 2582-7472

ShodhKosh: Journal of Visual and Performing Arts
July 2024 5(7), 16–26

# SIMPLIFIED MODELLING OF INDUCTION GENERATOR IN STATOR FLUX ORIENTED SYNCHRONOUS REFERENCE FRAME

Rishikesh Choudhary [1], Kumar Jyotiraditya [2], Dipo Mahto [3]

[1] Assistant Professor, Department of Electrical Engineering, Bhagalpur College of Engineering, Bhagalpur, Bihar, India
[2] Assistant Professor, Department of Mechanical Engineering, Bhagalpur College of Engineering, Bhaglapur, Bihar, India
[3] Professor and Head, Department of Physics, Bhagalpur College of Engineering, Bhagalpur, Bihar, India

**Corresponding Author**
Dipo Mahto, dipomahto@hotmail.com

**DOI**
10.29121/shodhkosh.v5.i7.2024.1774

**Funding:** This research received no specific grant from any funding agency in the public, commercial, or not-for-profit sectors.



## ABSTRACT

The selection of an appropriate reference frame is crucial for the accurate modeling of Doubly Fed Induction Generators (DFIGs). This paper presents a simplified approach to steady-state modeling of DFIGs using the Stator Flux-Oriented (SFO) Synchronous Reference Frame. The primary objective is to derive the steady-state characteristics of both directly grid-connected Squirrel Cage Induction Generators (SCIGs) and rotor-side controlled DFIGs. By leveraging the SFO reference frame, which ensures that all q-d transformed variables assume constant values, the voltage equations of a DFIG can be reduced from differential to algebraic equations, thus simplifying the analysis. The results demonstrate that the SFO reference frame provides a clear and close loop analytical solution for steady-state operating points, in contrast to alternative reference frames that could yield complex, highly coupled non-linear systems. This simplification is particularly advantageous as it aligns with the machine control framework used during transient periods. The steady-state solution obtained using the SFO reference frame is ideal for initializing control and analyzing both small-signal linear and large-signal transient disturbances, confirming its efficacy and suitability for practical applications.

**Keywords:** Stator Flux-Oriented (SFO), Reference Frame, Small-Signal Analysis, Small-Signal Linear and Large-Signal Transient Disturbances

## 1. INTRODUCTION

Over the past few decades, renewable energy alternatives have attracted significant attention due to the severe depletion of conventional resources, rapidly growing energy demands in newly industrialized countries, and the environmental concerns resulting from unchecked emissions. The global energy crisis has been extensively studied in [1], and various alternative solutions have been proposed. A comprehensive bibliographic analysis of numerous studies in [2] offers insights into the future direction of renewable energy research. Researchers worldwide are striving to harness energy from green alternatives such as wind, solar, and tidal

sources. These alternatives not only produce zero carbon emissions but also have negligible fuel costs.

Among all renewable energy resources, wind and solar systems have seen the most significant advancements [3], [4]. The choice between these two technologies is often subjective, as each has its own strengths and limitations. In terms of reliability based on resource availability, wind energy conversion systems hold an advantage over solar energy systems, as power generation can occur both day and night, as long as wind is present. Wind energy conversion systems also require less space and investment, with faster payback periods compared to solar systems [5]. Moreover, wind power can be developed offshore, enabling large-scale implementation.

The most popular wind energy conversion topology utilizes the doubly fed induction generator (DFIG) which is nothing, but a wound rotor induction generator fed from stator as well as from rotor side. The stator of the DFIG is directly connected to the grid whereas rotor is connected to the grid via a back-to-back PWM convertor. This configuration is better than that using singly excited induction generator in terms of energy capture efficiency, power quality, shaft fatigue problems. Currently this DFIG based semi-variable speed WECSs are covering up to almost 50% of the total worldwide commercial installations [6]. In SCIG or DFIG based WECSs operated by low-speed turbine the use of gearbox is inevitable because a multi-pole low-speed IG is not technically feasible [7]. Despite of the problems associated with gearboxes the DFIGs still have some advantage over other counterparts. One of the main advantages being the fairly reduced size converter for limited speed range control, as the converter need to handle only the slip power. For example if the required speed variation, be % around synchronous speed, the converter required rating shall be 30 % of machine rating [8]. Reduced converter size results into lower initial cost, lower convertor power loss, and lower filter size in comparison to the full-scale configuration where the full capacity converter shall be used. For the large or small signal model of WECSs, the initial steady state solution must be known beforehand [9]. In this paper, the steady state behaviour of direct grid connected SCIG and rotor side controlled DFIG shall be obtained.

## 2. MODELLING OF DFIG

In synchronously rotating reference frame, all q-d transformed variables assumes constant values therefore the voltage equations (differential equations) of a DFIG can be reduced into the following algebraic equations

$$v_{qs}^{e} = r_s i_{qs}^{e} + \omega_e \lambda_{ds}^{e} + p\lambda_{qs}^{e} \tag{1a}$$

$$\Rightarrow v_{qs}^{e} = r_s i_{qs}^{e} + \omega_e L_{ss} i_{ds}^{e} + \omega_e L_M i_{dr}^{\prime e} \tag{1b}$$

$$v_{ds}^{e} = r_s i_{ds}^{e} - \omega_e \lambda_{qs}^{e} + p\lambda_{ds}^{e} \tag{2a}$$

$$\Rightarrow v_{ds}^{e} = r_s i_{ds}^{e} - \omega_e L_{ss} i_{qs}^{e} - \omega_e L_M i_{qr}^{\prime e} \tag{2b}$$

$$v_{qr}^{\prime e} = r_r^{\prime} i_{qr}^{\prime e} + (\omega_e - \omega_r)\lambda_{dr}^{\prime e} + p\lambda_{qr}^{\prime e} \tag{3a}$$

$$\Rightarrow v_{qr}^{\prime e} = r_r^{\prime} i_{qr}^{\prime e} + \omega_e s L_{rr}^{\prime} i_{dr}^{\prime e} + \omega_e s L_M i_{ds}^{e} \tag{3b}$$

$$v_{dr}^{\prime e} = r_r^{\prime} i_{dr}^{\prime e} - \omega_e s \lambda_{qr}^{\prime e} + p\lambda_{dr}^{\prime e} \tag{4a}$$

$$\Rightarrow v_{dr}^{\prime e} = r_r^{\prime} i_{dr}^{\prime e} - \omega_e s L_{rr}^{\prime} i_{qr}^{\prime e} - \omega_e s L_M i_{qs}^{e} \tag{4b}$$

In the case of an SCIG the rotor voltage is zero, therefore for a given set of values of, and, the above system of equations of four unknowns: , and , can be solved at different possible values of the slip "s" (Equation 5).

$$\begin{bmatrix} i_{qs}^{e} \\ i_{ds}^{e} \\ i_{qr}^{'e} \\ i_{dr}^{'e} \end{bmatrix} = \begin{bmatrix} r_s & \omega_e L_{ss} & 0 & \omega_e L_M \\ -\omega_e L_{ss} & r_s & -\omega_e L_M & 0 \\ 0 & s\omega_e L_M & r_r' & s\omega_e L_{rr}' \\ -s\omega_e L_M & 0 & -s\omega_e L_{rr}' & r_r' \end{bmatrix}^{-1} \begin{bmatrix} v_{qs}^{e} \\ v_{ds}^{e} \\ 0 \\ 0 \end{bmatrix} \tag{5}$$

The obtained values are then used to find the electromagnetic torque, the stator active power and the stator reactive power at different rotor speed.

For the direct grid connected SCIG is operating under rated steady state condition, the values of, and have been taken as follows

$$\omega_e = \omega_{rated} \tag{6}$$

$$v_{qs}^{e} = \sqrt{2} v_s \cos(\alpha) \tag{7}$$

$$v_{qs}^{e} = -\sqrt{2} v_s \sin(\alpha) \tag{8}$$

Here is the rated stator frequency, is the rated per-phase stator voltage. The variable can be assigned any arbitrary value as it depends on the initial value of the applied instantaneous voltage and the initial location of the reference frame- (which can always be chosen arbitrarily). It has been seen, as expected that all the steady state characteristics of IM is independent of the value of. The parameters of the machine are given in appendix-I.

Since the machine control is in general executed within the Stator Flux-Oriented (SFO) reference frame, it is both logical and consistent to derive the steady-state performance characteristics in this same reference frame. Analogous to the transient control scenario, the q-axis component of the stator flux linkage will likewise be maintained at zero in the steady-state condition. (i.e.). It will be evident subsequently that employing this reference frame facilitates a more profound understanding of the underlying physical phenomena.

## 3. STATOR FLUX-ORIENTED (SFO) SYNCHRONOUS REFERENCE FRAME

The proper choice of the reference frame is of prime importance for modelling a doubly fed induction generator. In steady-state operation, the rotational speed of the Stator Flux-Oriented (SFO) reference frame coincides with the synchronous speed, while its initial spatial position at time zero is determined exclusively by the zero crossing of the instantaneous flux linkage in stator phase-A. The instantaneous spatial orientation of the SFO reference frame in the steady state can be mathematically expressed by Equation 9.

$$\theta = \tan^{-1}\left( \frac{\sqrt{2}\Lambda_s \cos(\omega_e t + \phi_{e\lambda s}(0))}{-\sqrt{2}\Lambda_s \sin(\omega_e t + \phi_{e\lambda s}(0))} \right) \tag{9a}$$

$$\Rightarrow \theta = \omega_e t + \phi_{e\lambda s}(0) - \frac{\pi}{2} \tag{9b}$$

Therefore, the time-zero spatial location of the SFO reference frame under steady state can be given as follows

$$\theta(0) = \phi_{e\lambda s}(0) - \frac{\pi}{2} \tag{10}$$

Since the speed of the Stator Flux-Oriented (SFO) reference frame is same as that of the synchronous reference frame, it may be aptly designated as the "SFO synchronous reference frame" in the steady state. However, it is distinct from the conventional synchronous reference frame, wherein the spatial position at time zero is arbitrarily defined. As with any synchronous reference frame, all d-q variables within the SFO reference frame attain constant values under steady-state conditions, and consequently, their time derivatives can be set to zero.

The superscript “e” has been used in a manner analogous to its use in the synchronous reference frame, reflecting the fact that the rotational speed of this frame is same as that of the synchronous reference frame.

$$v_{qs}^{e} = \sqrt{2} v_s \cos(\gamma) \tag{11}$$

$$v_{ds}^{e} = -\sqrt{2} v_s \sin(\gamma) \tag{12}$$

$$\gamma = \phi_{evs}(0) - \theta(0) \tag{13a}$$

$$\Rightarrow \gamma = \phi_{evs}(0) - \phi_{e\lambda s}(0) + \pi/2 \tag{13b}$$

Referring to Equations (11) and (12)

$$(v_{qs}^{e})^2 + (v_{ds}^{e})^2 = 2.v_s^2 \tag{14}$$

Here, denotes the per-phase stator RMS voltage, which, in the case of a Doubly-Fed Induction Generator (DFIG), is equivalent to the grid voltage. In the steady-state regime, the qd-axis stator and rotor voltage equations can be reformulated by neglecting the dynamic terms.

$$v_{qs}^{e} = r_s i_{qs}^{e} + \omega_e \lambda_{ds}^{e} + p\lambda_{qs}^{e} \tag{15a}$$

$$\Rightarrow v_{qs}^{e} = \frac{r_s L'_{rr}}{D} \lambda_{qs}^{e} - \frac{r_s L_M}{D} \lambda_{qr}^{\prime e} + \omega_e \lambda_{ds}^{e} \tag{15b}$$

$$\Rightarrow v_{qs}^{e} = k_1 \lambda_{qs}^{e} - k_2 \lambda_{qr}^{\prime e} + \omega_e \lambda_{ds}^{e} \tag{16}$$

$$\Rightarrow v_{qs}^{e} = -k_2 \lambda_{qr}^{\prime e} + \omega_e \lambda_{ds}^{e}$$

$$\Rightarrow \sqrt{2} v_s \cos(\gamma) = -k_2 \lambda_{qr}^{\prime e} + \omega_e \lambda_{ds}^{e} \tag{17}$$

$$v_{ds}^{e} = r_s i_{ds}^{e} - \omega_e \lambda_{qs}^{e} + p\lambda_{ds}^{e} \tag{18a}$$

$$\Rightarrow v_{ds}^{e} = \frac{r_s L'_{rr}}{D} \lambda_{ds}^{e} - \frac{r_s L_M}{D} \lambda_{dr}^{\prime e} - \omega_e \lambda_{qs}^{e} \tag{18b}$$

$$\Rightarrow v_{ds}^{e} = k_1 \lambda_{ds}^{e} - k_2 \lambda_{dr}^{\prime e} - \omega_e \lambda_{qs}^{e}$$

$$\Rightarrow v_{ds}^{e} = k_1 \lambda_{ds}^{e} - k_2 \lambda_{dr}^{\prime e} \tag{19}$$

$$\Rightarrow -\sqrt{2} v_s \sin(\gamma) = k_1 \lambda_{ds}^{e} - k_2 \lambda_{dr}^{\prime e} \tag{20}$$

$$v_{qr}^{\prime e} = r'_r i_{qr}^{\prime e} + (\omega_e - \omega_r) \lambda_{dr}^{\prime e} + p\lambda_{qr}^{\prime e} \tag{21a}$$

$$\Rightarrow v_{qr}^{\prime e} = k_3 \lambda_{qr}^{\prime e} - k_4 \lambda_{qs}^{e} + (\omega_e - \omega_r) \lambda_{dr}^{\prime e} \tag{21b}$$

$$\Rightarrow v_{qr}^{\prime e} = k_3 \lambda_{qr}^{\prime e} + (\omega_e - \omega_r) \lambda_{dr}^{\prime e} \tag{22}$$

$$v_{dr}^{\prime e} = r'_r i_{dr}^{\prime e} - (\omega_e - \omega_r) \lambda_{qr}^{\prime e} + p\lambda_{dr}^{\prime e} \tag{23}$$

$$\Rightarrow v_{dr}^{\prime e} = k_3 \lambda_{dr}^{\prime e} - k_4 \lambda_{ds}^{e} - (\omega_e - \omega_r) \lambda_{qr}^{\prime e} \tag{24}$$

The torque expression can be reformulated as follows:

$$\Rightarrow \lambda_{ds}^{e}\lambda'^{\,e}_{qr} = -\frac{4D}{3PL_M}T_e^* \tag{25}$$

In accordance with mechanical equilibrium

$$\Rightarrow \lambda_{ds}^{e}\lambda'^{\,e}_{qr} = K_O\omega_r^2 \text{ for } \omega_r \le \omega_{r,rated} \text{ (Sub-Rated Regime)} \tag{26}$$

$$= \frac{K_O\omega_{r,rated}^3}{\omega_r} \text{ for } \omega_r \ge \omega_{r,rated} \text{ (Rated Regime)}$$

By applying Equations (16) and (19) the stator reactive power equation can be reformulated as follows

$$Qs^* = \frac{3}{2}.\left(v_{qs}.i_{ds} - v_{ds}.i_{qs}\right)$$

$$\Rightarrow Q_S^* = \frac{3\omega_e}{2r_s}\lambda_{ds}^{e}(k_1\lambda_{ds}^{e} - k_2\lambda'^{e}_{dr}) \tag{27}$$

The system of five simultaneous equations—Equations (16), (19), (14), (26), and (27)—can be solved to determine the five unknowns: and.

The resulting values should then be used in the rotor voltage equations (22) and (24) to compute the desired rotor voltages and. Although the stator of the DFIG is directly connected to the grid, the stator q-d components and cannot be assumed to be constant or independent of speed due to the use of the Stator Flux-Oriented (SFO) reference frame, which differs partially from the conventional synchronous reference frame. Consequently, these quantities are considered unknown, though they must always satisfy the condition specified by Equation (14).

By substituting Equation (19) into Equation (27),

$$Q_S^* = \frac{3\omega_e v_{ds}^{e}}{2r_s}\lambda_{ds}^{e} \Rightarrow v_{ds}^{e} = \frac{2r_sQ_S^*}{3\omega_e\lambda_{ds}^{e}} \tag{28}$$

From Equations (14) and (28), it follows that

$$v_{qs}^{e} = \left[2v_s^2 - \left[\frac{2r_sQ_S^*}{3\omega_e\lambda_{ds}^{e}}\right]^2\right]^{1/2} \tag{29}$$

From equations 16 and 29,

$$\left[2v_s^2 - \left[\frac{2r_sQ_S^*}{3\omega_e\lambda_{ds}^{e}}\right]^2\right]^{1/2} = -k_2\lambda'^{e}_{qr} + \omega_e\lambda_{ds}^{e}$$

$$\left[2v_s^2\lambda_{ds}^{e\,2} - \left[\frac{2r_sQ_S^*}{3\omega_e}\right]^2\right]^{1/2} = -k_2\lambda_{ds}^{e}\lambda'^{e}_{qr} + \omega_e\lambda_{ds}^{e\,2} \tag{30}$$

From equations 30 and 26 (under sub-rated regime),

$$\left[2v_s^2\lambda_{ds}^{e\,2} - \left[\frac{2r_sQ_S^*}{3\omega_e}\right]^2\right] = \left(-k_2K_O\omega_r^2 + \omega_e\lambda_{ds}^{e\,2}\right)^2 \tag{31}$$

Assuming $\lambda_{ds}^2 = X$

$$\Rightarrow X^2 + (B/A)X + (C/A) = 0 \tag{32}$$

For sub-rated regime the coefficients of equation (32) can be expressed as follows

$$A = \omega_e{}^2$$

$$B = -2\omega_e k_2 K_O \omega_r^2 - 2v_s^2$$

$$C = (k_2 K_O)^2 \omega_r^4 + \left[\frac{2r_s Q_S^*}{3\omega_e}\right]^2$$

Generally, it is found that under normal operating conditions the term "C/A" is negligibly small in comparison to B/A, therefore the above equation can lead into the following solution for "X,"

$$X = \frac{-B}{A} = \frac{2k_2 K_O \omega_r^2}{\omega_e} + 2\left(\frac{v_s}{\omega_e}\right)^2 \tag{33}$$

Applying the assumption over the above Equation 33, the expression for the d-axis stator flux linkage in sub-rated regime can be given as follows

$$\Rightarrow \lambda_{ds}^e = \left[\frac{2k_2 K_O \omega_r^2}{\omega_e} + 2\left(\frac{v_s}{\omega_e}\right)^2\right]^{1/2} \tag{34}$$

It is evident that the steady-state value of the d-axis stator flux linkage exhibits minimal sensitivity to variations in the stator reactive power command. This simplified formulation arises from the assumption that the term C/A is negligibly small compared to the term B/A. While this assumption is generally valid in most practical scenarios, it may not hold if the stator frequency is exceptionally low.

For the rated operating regime, the coefficient in Equation (32) can be revised and expressed as follows:

$$A = \omega_e{}^2$$

$$B = -\frac{2k_2 K_O \omega_e \omega_{r,rated}^3}{\omega_r} - 2v_s^2$$

$$C = \left[\frac{k_2 K_O \omega_{r,rated}^3}{\omega_r}\right]^2 + \left[\frac{2r_s Q_S^*}{3\omega_e}\right]^2$$

It is observed that the value of C/A remains negligible compared to B/A Consequently, Equation (32) indicates that the expression for the d-axis stator flux linkage in the rated regime can be formulated as follows:

$$\Rightarrow \lambda_{ds}^e = \left[\frac{2k_2 K_O \omega_{r,rated}^3}{\omega_e \omega_r} + 2\left(\frac{v_s}{\omega_e}\right)^2\right]^{1/2} \tag{35}$$

This equation showes that, at the rated regime, the steady-state d-axis stator flux linkage decreases with increasing steady-state rotor speed.

## 4. APPROXIMATED STEADY STATE SOLUTION

Under steady state using and applying equation (34) & (35) into Equations-(28) & (29), the steady state d-axis and the steady state q-axis stator voltages can be approximately expressed as follows in the sub-rated and the rated regime

$$v_{ds}^{e} = \frac{2r_s Q_S^*}{3}\left[2k_2 K_O \omega_r^2 + 2v_s^2\right]^{-1/2} \tag{36a}$$

For (Sub-rated regime)

$$= \frac{2r_s Q_S^*}{3}\left[\frac{2k_2 K_O \omega_{r,rated}^3}{\omega_r} + 2v_s^2\right]^{-1/2} \tag{36b}$$

For (Rated regime)

$$\Rightarrow v_{ds}^{e} = \frac{\sqrt{2}r_s Q_S^*}{3v_s} \tag{37}$$

The above approximation stems from the fact that under practical cases.

$$v_{qs}^{e} = \left[2v_s^2 - \left[\frac{\sqrt{2}r_s Q_S^*}{3v_s}\right]^2\right]^{1/2} \tag{38}$$

For the practical range of parameter and operating conditions, the following approximation holds good.

$$Q_S^* << \frac{3v_s^2}{r_s} \tag{39}$$

This approximation shall result into the following simplified results for the steady state q-axis stator voltage

$$v_{qs}^{e} \approx \sqrt{2}v_s \tag{40}$$

In practical cases, the steady state d-axis component of stator voltage is also negligibly small in comparison to its q-axis counterpart.

$$v_{ds}^{e} = \frac{\sqrt{2}r_s Q_S^*}{3v_s} \tag{41}$$

Since is very small, the equation (19) reduces into the following equation

$$k_1 \lambda_{ds}^{e} = k_2 \lambda_{dr}^{re} \Rightarrow \lambda_{dr}^{re} = \frac{k_1}{k_2}\lambda_{ds}^{e} \tag{42}$$

It can be seen that the steady state d-axis rotor flux linkage is also almost same for all speeds (& reactive power settings) in the same way as is the d-axis stator flux linkage.

By using (26) and (35) in Sub-Rated Regime

$$\lambda_{qr}'^{\,e} = \frac{K_O \omega_e}{\sqrt{2}v_s}\omega_r^2 \tag{43}$$

Whereas in Rated Regime

$$\lambda'^{\,e}_{qr} = \frac{K_O \omega_e \omega^3_{r,rated}}{\sqrt{2} v_s} \cdot \frac{1}{\omega_r} \tag{44}$$

## 5. RESULT AND DISCUSSION

The equations (34) and (35) have the major contributions to makes it evident that, in the steady-state sub-rated regime, the d-axis stator flux linkage increases with rotor speed and at the rated regime, the steady-state d-axis stator flux linkage decreases with increasing steady-state rotor speed respectively. The relationship is quadratic, reaching its peak at the rated rotor speed. However, in practical scenarios, these variations are minimal, leading to the d-axis stator flux linkage remaining relatively constant across different rotor speeds, provided the stator voltage magnitude and frequency are maintained at their rated values (Figure 1).

The value of can be put into the Equations 28 and 29 to obtain and in sub-rated and rated regime (Figure-1). With these variables (, and) known, we can obtain all other unknown variables of the voltage-equations 16, 19, 22 and 24, leading to the complete steady-state solution (Figure-2 and 3).

**Figure 1**

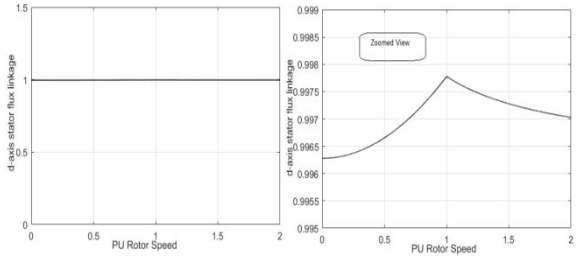


**Figure 2**

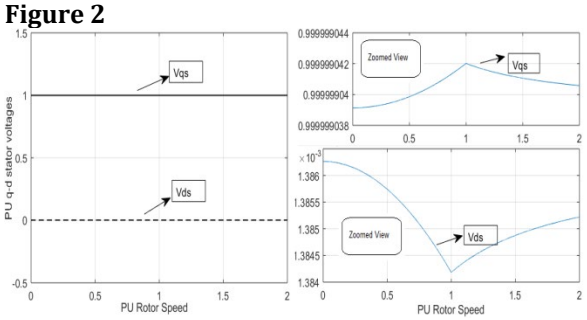


**Figure 3**

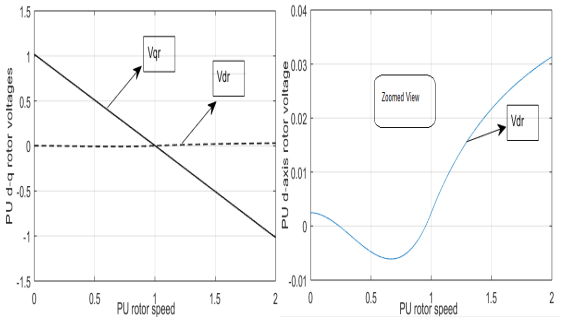

By using the expressions of the flux linkages, the equations (43), (42), (43) and (44) all currents can be found with the help of the equation-(31). The speed dependence of the different steady state stator and rotor flux currents has been depicted in Figure 4.

**Figure 4**

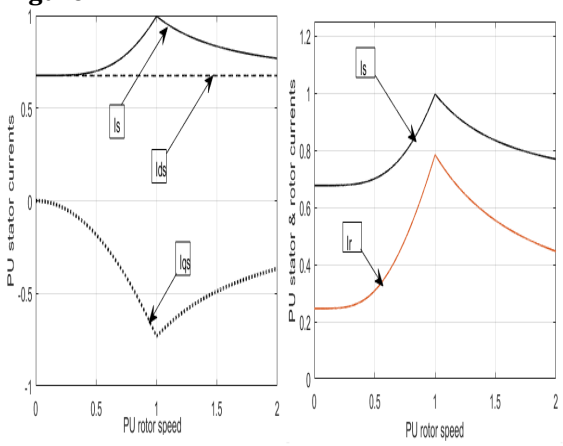


## 6. CONCLUSION

It can be concluded that the practical simplifications combined with the use of the Stator Flux-Oriented (SFO) reference frame have led to a straightforward analytical solution for the steady-state operating points. In contrast, addressing the same problem in an alternative reference frame would likely result in a complex, highly coupled non-linear system of equations. Employing the SFO reference frame for determining steady-state characteristics is particularly logical, given that the machine control framework during transient periods is also defined in this reference frame. Since the steady-state solution will be utilized for initializing the control and analysis of small-signal linear or large-signal transient disturbances, the SFO reference frame is thus the most appropriate choice.

## APPENDIX

$$k_1 = \frac{r_s L'_{rr}}{D},\ k_2 = \frac{r_s L_M}{D},\ k_3 = \frac{r'_r L_{ss}}{D},\ k_4 = \frac{r'_r L_M}{D}$$

Turbine-Parameters

$$C_P(\lambda,\beta) = 0.5176\left(\frac{116}{\lambda_i} - 0.4\beta - 5\right).\exp\left(-\frac{21}{\lambda_i}\right) + 0.0068\lambda$$

Where, $\frac{1}{\lambda_i} = \left(\frac{1}{\lambda + 0.08\beta}\right) - \left(\frac{0.035}{\beta^3 + 1}\right)$

$\lambda_{opt} = 8.1$

$\beta_{opt} = 0$

$C_P\_\max = C_P(\lambda_{opt}, \beta_{opt}) = 0.48$

$v_w\_rated = 14\ \text{m/s}$

$\rho = 1.225$ Kg/m$^2$

$P_{WT\_rated} = 4.5MW$

$S\_rated = 5MVA$

$$P_{WT} = \frac{1}{2}\rho.\pi R^2.v_w^3.C_p(\lambda,\beta)$$

$$P_{WT\_rated} = \frac{1}{2}\rho.\pi R^2.v_{w\_rated}^3.C_{p\_\max}$$

$$P_{WT\_rated} = \frac{1}{2}\rho.\pi R^2.v_{w\_rated}^3.C_{p\_\max}$$

$$S\_rated = \frac{P_{WT\_rated}}{\gamma}$$

power clearance is given). For present work the value of has been assumed to be 0.9.

$$R = \sqrt{\frac{2P_{WT\_rated}}{\rho\pi v_{w\_rated}^3 C_{p\_\max}}}$$

$$\omega_{T\_rated} = \frac{\lambda_{opt} v_{w\_rated}}{R}$$

Machine Parameters

No of poles, P=4

Stator resistance, rs=0.000487 ohms

Rotor resistance, rr=1.18*rs

Magnetizing Reactance, XM=0.2908 ohms

Stator self-reactance, Xss=1.02*XM

Rotor Self reactance referred to stator=1.005*XM

Kopt=0.145131904949398Wsec2/electrical-rad2

DeqH= 300 N-m/ (elec-rad/sec)

keqH= 8500 N-m/ (elec-rad)

Rotor Inertia of the generator, JG=75 kg/ m$^2$

Turbine Inertia, J'WT =9*JG

Per unit formulation for turbine torque shall be as follows

$$T_{WT} = \frac{1}{2}\rho.\pi R^2.v_w^3.C_p(\lambda,\beta)\frac{1}{\omega_T}$$

$$(T_{WT})\_rated = \frac{S\_rated}{\omega_{bm}/n_{gb}} = \frac{S\_rated}{\omega_{T\_rated}/\alpha}$$

$$T_{WT\_pu} = \frac{\gamma}{\alpha}\frac{v_{w\_pu}^3 C_p(\lambda,\beta)}{C_{p\_\max}}\frac{1}{\omega_{WT\_pu}}$$

(Here, $\lambda = \frac{\omega_{T\_pu}}{v_{w\_pu}}\lambda_{opt}$).

$$T_{WT\_pu} = 0.9 \frac{v_{w\_pu}^3 C_p(\lambda, \beta)}{C_{p\_\max}} \frac{1}{\omega_{WT\_pu}}$$

Here, $K_O = \frac{2Dk_{opt}}{3L_M}$

## CONFLICT OF INTERESTS

None.


## ACKNOWLEDGMENTS

None.


## REFERENCES


Coyle et al. Understanding the Global Energy Crisis, Purdue University Press, 2014.

Guozhu Mao et al. Way forward For Alternative Energy Research: A Bibliometric Analysis During 1994â€“2013, Renewable and Sustainable Energy Reviews, Volume 48, P276-286, 2015.

Armaroli et al. Towards An Electricity-Powered World, Energy and Environmental Science, 4 (9) : 3193–3222. 2011.

Lins et al : The first decade : 2004 – 2014, 10 years of Renewable Energy Progress (INIS-FR--15-0639), France, 2014.

M. Liserre et al. Overview Of Multi-Mw Wind Turbines and Wind Parks, Ieee Trans. Ind. Electron., Vol. 58, No. 4, pp. 1081–1095, 2011.

L. H. Hansen et al., Conceptual Survey of Generators and Power Electronics for Wind Turbines. Roskilde, Denmark: Denmark Riso National Lab., Riso-R-1205(EN),2001.

H. Polinder et al., Trends in Wind Turbine Generator Systems, IEEE J. Emerg. Sel. Topics Power Electron., Vol. 1, No. 3, pp. 174–185, 2013.

Tianming Gu et al. Modeling and Small-Signal Stability Analysis of Doubly-Fed Induction Generator Integrated System, Global Energy Interconnection, Volume 6, Issue 4, p438-449,2023.